Protein:Colloid Conjugates for Surface Enhanced Raman Scattering: Stability and Control of Protein Orientation

Christine D. Keating, Kenneth M. Kovaleski, and Michael J. Natan*

Department of Chemistry, The Pennsylvania State University, University Park, Pennsylvania 16802

Received: June 22, 1998

Conjugates between cytochrome *c* (Cc) and colloidal Au particles have been prepared. These conjugates, purified by centrifugation/resuspension, provide a reproducible means of positioning a biomolecule analyte between two metal surfaces: the metal nanoparticle to which the biomolecule is bound and an aggregated Ag sol used as a substrate for surface enhanced Raman scattering (SERS). SERS spectra for Ag:Cc:Au sandwiches made by addition of Cc:Au conjugates to aggregated Ag show that the protein retains its native conformation. Conjugation of Cc to colloidal metal nanoparticles prior to exposure to the SERS substrate can be used as a means of controlling protein orientation with respect to the substrate. In addition, Cc molecules bound to 12-nm diameter Au nanoparticles prior to adsorption to aggregated Ag are more stable to changes in the orientation of the heme with respect to the surface and to surface-induced heme spin state conversion than adsorbed, free Cc. These experiments show that protein:Au conjugates offer benefits as reagents for protein SERS.

Introduction

This manuscript reports the preparation, characterization, and use of complexes (conjugates) between cytochrome *c* (Cc)[1] and colloidal Au nanoparticles as analytes for surface-enhanced Raman scattering (SERS).[2] The adsorption and conformation of proteins at metal surfaces is critical to many bioanalytical techniques involving transduction of protein-based signals for detection, including electrochemistry,[3] SERS,[2] surface plasmon resonance,[4] and quartz crystal microgravimetry.[5] Unfortunately, adsorption often leads to conformational changes, denaturation, or undesirable protein orientations with respect to the metal substrate.[6] To address these problems, metal surfaces have been modified with small molecules,[7] polymeric matrixes,[8] and colloidal Au particles.[9] Proteins bound to colloidal Au particles are known to retain biological activity, and have long been used as electron-dense biospecific stains for electron microscopy.[10] A previously unrecognized aspect of protein:colloid conjugate chemistry is the potential for use of colloidal Au particles as *delivery agents* for biomolecules. We describe herein the use of colloidal Au nanoparticles to control the orientation of cytochrome *c* (Cc) at a Ag SERS substrate. We show that the Cc in Cc:Au conjugates adsorbed to aggregated Ag retains its native conformation and is more stable to spin state changes over time than Cc that has been directly adsorbed to the Ag substrate.

In SERS, molecules adsorbed at roughened noble metal surfaces exhibit large (up to 10^6-fold) enhancements in vibrational spectral intensities. SERS has several advantages over resonance Raman (RR),[11] the vibrational spectroscopy most commonly employed in studies of biological chromophores. (i) Much smaller amounts of material are needed for SERS than for RR, because of the large increase in scattering, and because SERS interrogates principally the first molecular layer adsorbed to the enhancing substrate. (ii) The metal surfaces used in SERS are effective quenchers of fluorescence,[2,12] a substantial problem in RR experiments.[11] (iii) Since the SERS effect does not require resonant excitation of analyte chromophores, in principle any molecule can be studied by this technique. (iv) Laser wavelengths can be chosen to minimize fluorescence (e.g., 647.1 nm or near-infrared) or to decrease the possibility of sample damage. Alternately, resonant excitation can be coupled with SERS to give even greater enhancements than possible for either technique alone, along with selectivity for a chromophore.[13]

The failure of SERS, despite these advantages, to become ubiquitous in studies of proteins (and particularly those containing chromophores) is traceable to problems of protein denaturation and inherent irreproducibility of the roughened metal substrates necessary for enhancement in the Raman signal. Typical SERS substrates are electrochemically roughened Ag electrodes[14] or aggregated Ag hydrosols;[15] the biocompatibility of both substrates has been called into question.[16] To date, the best substrate for protein SERS appears to be aggregates of colloidal Ag particles made by citrate reduction of Ag^+. With this substrate, SERS has been used to show that adsorbed chlorocatechol dioxygenase retains activity.[17] In addition, cytochrome *c*[18] and several cytochromes P450[19] have been shown to retain native spin states while adsorbed to this type of surface.

Although citrate-reduced Ag colloids demonstrate excellent SERS enhancements and good biocompatability as compared to other roughened metal surfaces, they are composed of a variable mix of particle sizes and shapes.[15,20] This leads to irreproducibility in optical properties, aggregation properties, particle concentration, and total surface area of the resulting colloidal solutions. In contrast, monodisperse solutions of colloidal Au can be prepared having average diameters anywhere between 3 and 100 nm.[10,21] Colloidal Au nanoparticles conjugated to biological reporter molecules (e.g., antibodies, protein A) have long been used in biological samples as electron-dense tags for transmission electron microscopy (TEM), and methods for preparing Au particles and protein-coated particles

* To whom all correspondence should be directed (e-mail: natan@chem.psu.edu).

10.1021/jp982723z CCC: $15.00
Published on Web 11/03/1998

SCHEME 1: Preparation of Ag:Cc:Au Sandwiches for SERS

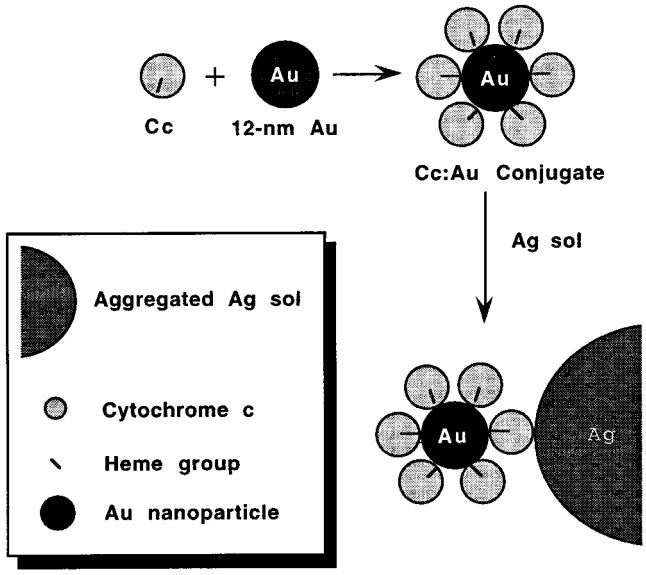

are well-developed.[10,22] In the vast majority of cases, proteins bound to colloidal Au (protein:Au conjugates) have been shown to retain their biological activity,[10,23] and the protein coverage on Au nanoparticles can be known, because the particle size and concentration are known.[23] Unfortunately, SERS enhancement factors for Au (with visible excitation) are substantially lower than for Ag;[24] accordingly, SERS intensities for previously described biomolecule:Au colloid conjugates have been relatively weak.[25]

Moreover, SERS has been of limited value for studies of proteins whose chromophores are "buried" within the structure of the protein, and thus ≥ 10 Å away from the metal substrate. For example, although the flavin cofactor alone gives excellent SERS scattering with resonant excitation,[26] little or no flavin signal is observed for glucose oxidase, a protein which contains this cofactor within the interior of its structure.[27] Cytochrome c_3, a protein composed of four subunits that each contain a c-type heme moiety, exhibits SERS scattering for only one of the heme groups—that which is closest to the Ag substrate surface.[28] This inability to observe SERS signals from even resonantly enhanced chromophores within proteins has been attributed to the distance between the cofactors and the metal surface. The electromagnetic field responsible for much of the enhancement seen in SERS drops off exponentially with distance from the surface.[2,29] Thus, the best enhancements are expected (and observed) for groups closest to the roughened metal substrate.

This paper and the subsequent article in this issue[30] describe a method that takes advantage of both the high SERS enhancements at aggregated (citrate-reduced) colloidal Ag and the reproducibility and control over protein surface coverage possible at protein:colloidal Au conjugates. By adsorbing protein-coated Au nanoparticles to colloidal Ag aggregates, a metal−protein−metal sandwich is prepared (Scheme 1). This article describes the preparation of protein:Au conjugates and the favorable consequences of their use vis à vis protein stability and control of protein orientation. The accompanying report presents evidence for heightened electromagnetic fields (and, thus, increased SERS enhancement factors) between the Ag and Au surfaces.[30] This approach effectively circumvents the normal distance dependence for SERS, and enables spectra to be acquired for a heme group located on the far side of the protein molecule (relative to the aggregated Ag). In both studies, cytochrome *c* (Cc) has been chosen as the model protein. This small, heme-containing, electron-transfer protein has been well-characterized by both RR[31] and SERS,[18,32−34] and a full assignment of the RR bands has been recently published.[35] Small shifts in the frequencies of Cc vibrational modes can be interpreted in terms of changes in the protein's conformation, oxidation state, or spin state.[31] Under certain conditions, this protein will change conformation and spin state upon binding to surfaces.[32,33] In addition, Cc has been crystallographically characterized,[36] and its adsorption to, and orientation at, several surfaces has been investigated.[37] Thus, Cc is ideally suited for investigations into the effects of using the metal−protein−metal sandwich approach to SERS.

Experimental Section

Materials. Horse heart cytochrome *c* (Sigma) was purified by affinity chromatography according to a literature protocol.[38] Au particles referred to as "60 nm" were purchased from Goldmark Biologicals, and they had a mean diameter of 62.8 nm. Poly(ethylene glycol) (PEG, MW 20 000) was from Fluka. All other reagents were acquired from the following suppliers: J. T. Baker, Aldrich, Acros, Sigma, or VWR. All H_2O was 18.2 MΩ, from a Barnstead Nanopure system. The pH of colloid solutions was determined using pH test strips (colorpHast) to within ± 0.5 pH unit.

Preparation of Colloidal Au, Ag, and Ag-Coated Au. Ag sols were prepared by aqueous reduction of $AgNO_3$ with trisodium citrate following the method of Lee and Meisel.[39] Ag sols prepared in this way are polydisperse, with average particle diameters typically ~30 nm and standard deviation of ±25 nm.[20] Colloidal Au 12 nm in diameter was prepared by citrate-reduction of $HAuCl_4$ as previously described.[21,40] Particles referred to in the text as "12-nm Au" were nearly spherical, with standard deviations in diameter <1.5 nm. Several preparations were used in this work. For each, particle sizes were determined from transmission electron micrographs (>250 particles) using the program NIH Image.[41]

Particles referred to as "40-nm Au" were prepared by using 12-nm Au particles as "seeds" for nucleation of larger particles.[42,43] One and one-half milliliters of 1% $HAuCl_4$ was added to 128 mL of H_2O, and this solution was heated to a boil, with rapid stirring. Then, a solution prepared by mixing 3.0 mL of 17.8 nM, 12-nm Au particles and 0.75 mL of 38.8 mM trisodium citrate was added all at once. The solution turned violet, followed by appearance of a red color. The solution was kept boiling and stirring vigorously for ~15 min after the addition of colloidal Au and trisodium citrate, during which time some H_2O was added to replace volume lost to evaporation. The final volume was 132 mL. Analysis of TEM images for 208 particles gave a major axis of 45.5 nm (±5.7 nm) and minor axis of 37.5 (±3.9 nm).

Ag-coated Au particles (henceforth Ag/Au) were prepared by using 12-nm Au particles as "seeds" for nucleation of Ag.[44] 50 mL of 17 nM, 12-nm Au particles was diluted with H_2O to 200 mL and heated, with rapid stirring. Upon boiling, 5.0 mL of 10 mM $AgNO_3$ was added rapidly from a syringe. At this time 1.0 mL of 1% trisodium citrate was also added. At 5 min intervals, additional 5.0 mL aliquots of 10 mM $AgNO_3$ were added, to a total of 30 mL. At the addition of the fourth aliquot of $AgNO_3$ solution, an additional 1.0 mL of 1% trisodium citrate was also added. The colloid solution was boiled and vigorously stirred throughout the additions, and for another 15 min, after which it was removed from heat and stirred until cooled. The resulting solution had an absorbance maximum at 392 nm, with

an absorbance of 1.7 after dilution 1:10 with H_2O. TEM analysis of these particles showed the presence of large (14−25-nm diameter) spheroidal particles and tiny particles (4−8 nm diameter). The absence of any 12-nm particles indicated that all the Au nanoparticles had been coated with Ag, yielding the larger particles. It appears that nucleation of Ag in solution led to the formation of the tiny particles.

Preparation of Au:Cc Conjugates. Cc:Au colloid conjugates[45] were prepared using horse heart ferricytochrome *c* (Fe^{3+}) and 12-nm diameter colloidal Au. The binding of Cc to colloidal Au particles was followed by a flocculation assay.[10,22] In this assay, increasing concentrations of protein were added to otherwise identical aliquots of Au hydrosol. Then, an aggregating agent (NaCl) was added to each solution. The amount of Cc necessary to prevent aggregation by NaCl was determined using optical spectra of the Au sol as indicator of aggregation. To prepare Cc:Au conjugates, a 10−50% excess of the minimum stabilizing concentration of Cc was added to a phosphate-buffered, pH 9.5 (±0.5) solution of Au sol. The solution was mixed gently and allowed to react for a few minutes before centrifugation in a Fisher Scientific Model 235C microcentrifuge for 15 min at 13600*g*. The supernatant was removed and the (soft) pellet resuspended in H_2O. Protein:colloid conjugates were stored at 4 °C when not in use. Under these conditions, Cc:Au(12-nm) samples were stable for several months.

Cytochrome *c* conjugates made with Ag-coated Au nanoparticles (Cc:Ag/Au) were prepared in a similar fashion. The saturating [Cc] was determined by a flocculation assay. Low-coverage Cc:Ag/Au conjugates were prepared by addition of 21% of the stabilizing [Cc], and 110% of the stabilizing [Cc] was used in preparing the high-coverage conjugates. Both samples were prepared at pH 9.5 ± 0.5. The resulting Cc:Ag/Au conjugates were purified by centrifugation and resuspension in H_2O. Some aggregation (evidenced by a color change from yellow/brown to a cloudy orange/brown color) was observed within 2 min of resuspension of conjugates, after which no further change was observed. All SERS spectra were acquired after this color change occurred.

SERS Acquisition. Typical SERS samples were prepared as follows: 500 μL of Ag or Au sol was aggregated by addition of 5 μL of 5 M NaCl, after which 50 μL of protein or protein colloid conjugate was added immediately, followed by 50 μL of 1% agarose (Biorad, low-melt). The agarose was kept liquid just above the gel point on a hot plate prior to use. SERS samples were then transferred to borosilicate glass culture tubes for immediate spectral acquisition. Samples were freshly prepared for each spectrum; all spectra were acquired at room temperature.

Power (10−100 mW) (measured at the sample with a Coherent Fieldmaster power meter equipped with an LD3 head) from a Coherent Innova Spectrum laser (mixed Ar^+/Kr^+) at 568.2 and 514.5 nm was used in SERS studies. Scattered light was collected in a backscattering geometry and focused into a SPEX 1877 triple monochromator fitted with either a 1200 or an 1800 grooves/mm grating in the spectrograph stage and two 600 grooves/mm gratings in the filter stage. Detection was accomplished using a CCD detector cooled to 140 K. The spectrometer was calibrated using imidazole as a frequency standard prior to each set of experiments, and was recalibrated whenever the excitation wavelength was changed.

Results and Discussion

Preparation of Protein:Colloid Conjugates. The concentration of Cc necessary to coat each Au nanoparticle in a 17.8 nM solution of colloidal Au was determined by finding the minimum Cc concentration capable of preventing electrolyte-induced aggregation of the Au sol. The surface plasmon resonance of isolated Au particles is at ∼520 nm.[46] Addition of electrolytes to Au hydrosols causes particle flocculation due to screening of the repulsive double layer charges that normally stabilize them,[47] leading to the appearance of a broad absorbance at long wavelengths (∼650 nm). This feature increases in intensity and/or broadens and red shifts with increasing aggregation.[48] Flocculation can be prevented by adsorption of stabilizers, such as polymers or proteins, to the sol; these large adsorbates cause steric repulsions between the particles. The amount of stabilizer necessary to prevent aggregation upon the addition of electrolyte can be determined from a flocculation assay.[10,22]

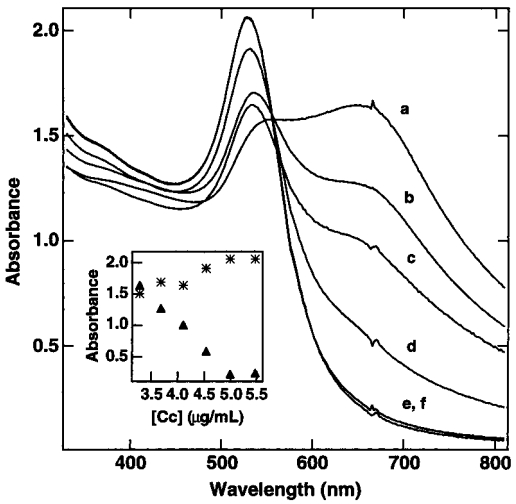

Figure 1. Flocculation data for Cc on 12-nm diameter colloidal Au. 500 μL of 1.5 M NaCl was added to 3.07 mL of 12 M, 12-nm Au particles containing varying concentrations of Cc: (curve a) 3.3 μg/mL, (curve b) 3.7 μg/mL, (curve c) 4.1 μg/mL, (curve d) 4.5 μg/mL, (curve e) 5.0 μg/mL, and (curve f) 5.5 μg/mL. Spectra were taken 15 min. after addition of NaCl. (Inset) Absorbance at 520 nm (∗) and at 650 nm (▲) vs [Cc].

Figure 1 shows flocculation data for increasing concentrations of Cc in aliquots of 12-nm Au nanoparticles. pH 9.5 was chosen for these experiments, since at higher pH the bare Au sol is unstable, and at lower pH the Cc is able to cross-link Au particles, causing aggregation. At pH 9.5, Cc is expected to bind to the negatively charged Au nanoparticles[49] through its lysine-rich heme pocket (at lower pH, a second, weakly positive patch on the opposite side of the protein also binds Au). The sample in spectrum a contains only 3.3 μg/mL Cc, which is insufficient to prevent aggregation upon addition of NaCl. Lesser amounts of aggregation (lower absorbance at ∼650 nm) are visible as [Cc] is increased, until, at 5.0 μg/mL, no further change is observed, and the spectrum is very similar to that of isolated Au nanoparticles.[50] The inset to Figure 1 plots sample absorbance at 520 and 650 nm versus [Cc]. The lowest ratio of Cc to Au nanoparticles that prevented aggregation in this experiment was ∼30 Cc per Au particle. This result is consistent with ∼0.6 monolayers of 34-Å diameter spheres packed around each of the 12-nm diameter Au particles, assuming that no Cc remained free in solution. In other flocculation studies of Cc added to 12-nm Au, values as high as ∼50 Cc/Au (a full monolayer) were obtained; the results are highly dependent on the pH of the colloid solution, with greater stabilization occurring at higher pH. Note that less than a

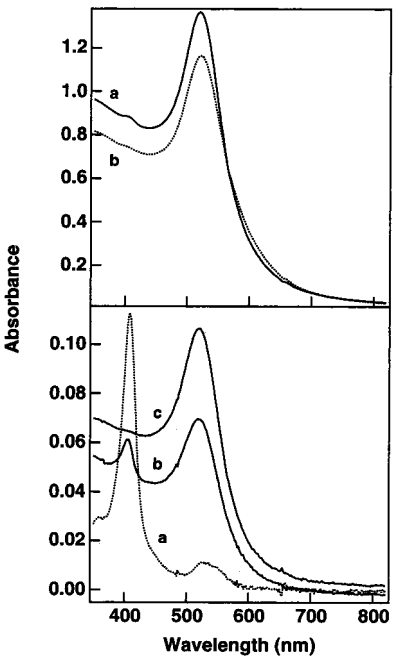

Figure 2. (Top) Optical spectra for conjugates of Cc with 12-nm diameter colloidal Au prior to centrifugation (curve a) and after centrifugation and resuspension twice (curve b). (Bottom) Optical spectra for: 1.4×10^{-6} M Cc (curve a) and supernatants from the first (curve b) and second (curve c) centrifugation of Cc:Au.

monolayer of protein is effective at (sterically) inhibiting particle flocculation.

Cytochrome *c*:12-nm diameter Au nanoparticle conjugates were prepared by adding a slight excess of Cc (110% of the stabilizing concentration, as determined by flocculation) to colloidal Au at pH ~9.5. The optical spectrum for this material is shown in the upper panel of Figure 2, spectrum a. Excess Cc was removed by centrifugation of the conjugate solution to produce a pellet (Au:Cc and any free Au), which was then resuspended in buffer; this procedure was done once or twice. An optical spectrum of the final Cc:Au conjugate solution is shown in the upper panel of Figure 2, spectrum b. The decreased absorbance shows that some Au has been lost in the centrifugation step. In addition, there is only slight broadening of the peak, indicating that very little, if any, aggregation has occurred. Optical spectra of the first and second supernatants are shown in the lower panel of Figure 2, along with a spectrum of 1.36×10^{-6} M Cc. Some Au nanoparticles remain in both supernatants, as evidenced by the absorbance at ~520 nm (note that the pellet is soft, thus a small amount of Cc:Au tends to be lost with the supernatant as it is decanted—this amount is greater in trace c than trace b). More importantly, optical spectra for the supernatants also indicate not only that some excess Cc was lost in the first round of centrifugation but that much less Cc was present in the second supernatant (as evidenced by the smaller peak at 400 nm in the second supernatant).

Cc:Au conjugates were also prepared using larger Au nanoparticles, with polydisperse Ag nanoparticles,[30] and with Ag-coated Au nanoparticles. For 40-nm and 60-nm diameter, spherical, monodisperse colloidal Au, flocculation assays showed essentially quantitative binding of Cc, as was observed for 12-nm Au (Supporting Information). For the 60-nm Au flocculation, the long-wavelength absorbance feature is not as intense in corresponding spectra as for the 12-nm and 40-nm flocculation assays. However, the decrease in absorbance at ~534 nm is also indicative of aggregation. Flocculation assays gave ~1730 Cc/40-nm Au (0.8 times that predicted value for a monolayer), and ~1850 Cc/60-nm Au particle (1.3 times that predicted value for a monolayer). The higher [Cc] required to stabilize the 60-nm Au particles may be related to the presence of polymeric stabilizers in this solution;[51] some of the Cc may have bound to these stabilizers rather than the Au. Cc:Au conjugates were prepared with 40- and 60-nm Au particles; these conjugates were similar to Cc:Au prepared using 12-nm Au, except for exhibiting a reduced stability that is typically associated with larger Au particles.[52] After pelleting, Cc:Au can be resuspended in almost arbitrarily small volumes to prepare more concentrated solutions. This is particularly helpful for conjugates prepared with the very dilute 40- and 60-nm Au particles.

CHART 1: Three Geometries for Cc SERS Spectra on Aggregated Ag Sols

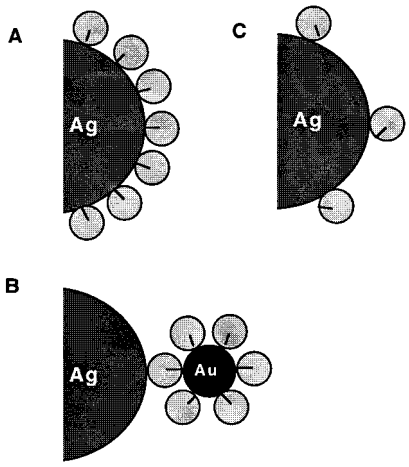

SERS of Metal−Cc−Metal Sandwiches. Ag:Cc:Au sandwiches are prepared by addition of Cc:Au conjugates to aggregated colloidal Ag as shown in Scheme 1. The two basic types of Cc SERS samples investigated in this manuscript are illustrated in Chart 1 **A** and **B**. In both cases, the Ag nanoparticle in the diagram is a gross oversimplification of the actual Ag surface. In fact, the Ag is present as large, fractal aggregates of polydisperse Ag nanoparticles (mean diameter = 30 nm). **A** represents Cc directly adsorbed to aggregated Ag sol (Ag:Cc), while **B** is Cc:Au adsorbed to the aggregated colloidal Ag (Ag:Cc:Au). Key aspects of these two geometries are the location of Cc's heme group relative to the Ag substrate (near the SERS-active Ag for **A**, distant in **B**), and the orientation of the heme plane relative to the surfaces. Both colloidal Ag and Au particles are negatively charged, due to adsorbed citrate[53] and chloride ions present during their preparation. Previous studies have shown that Cc adsorbs to negatively charged surfaces with the heme group very close to the surface;[37] at high Cc coverages, the heme is oriented close to the surface normal, while at low coverages, the heme-surface angle decreases.[18] Also important is the location of a second, weaker positive patch on the opposite side of the Cc molecule, facilitating "sandwich" formation. Previously reported SERS spectra for Cc derive almost exclusively from vibrations of the heme chromophore,[18,31−34] which is covalently bound to the protein through the porphyrin substituents by two cysteine residues and by the Fe's two axial ligands, histidine and methionine.

The protein-colloid literature stresses the importance of additional polymeric adsorbates to stabilize conjugates, by occupying any sites left available on Au particles after binding the protein of interest.[10,22] Such stabilizers are typically added in large excess prior to centrifugation, and again in the

TABLE 1: Band Locations and Assignments for SERS Spectra of Ag:Cc and Ag:Cc:Au

$\lambda_{ex} = 514.5$ nm		$\lambda_{ex} = 568.2$ nm			
Ag:Cc[a] (cm^{-1})	Ag:Cc:Au[b] (cm^{-1})	Ag:Cc (cm^{-1})	Ag:Cc:Au (cm^{-1})	mode (refs 11a and 31)	symmetry
1316	1317	1318	1318	ν_{21}	A_{2g}
1373	1372	1372	1372	ν_4	A_{1g}
1407	1407	1407	1404	ν_{20}	A_{2g}
1450	1455				
		1489	1491		
1505	1504			ν_3	A_{1g}
1567	1567	1570	1570	ν_{11}	A_{2g}
1585	1584	1584	1585	ν_{19}	A_{1g}
1641	1641	1641	1642	ν_{10}	B_{1g}

[a] Horse heart ferricytochrome *c* directly adsorbed to aggregated colloidal Ag. [b] Conjugates of horse heart ferricytochrome *c* with 12 nm diameter colloidal Au nanoparticles prepared and purified prior to adsorption to aggregated colloidal Ag.

resuspension buffer. In our initial studies, we followed these protocols[10,22] in preparing Cc:Au. However, the stabilizers [in particular, poly(ethylene glycol) (PEG), fish gelatin, and bovine serum albumin] exhibit weak SERS spectra when adsorbed to colloidal Ag aggregates, and are able to compete effectively with Cc:Au for adsorption sites on Ag aggregates due to their high solution concentration. This had the effect of masking SERS signal from the desired analyte. For example, SERS from the heme chromophore is observed for Cc directly adsorbed to aggregated colloidal Ag (Ag:Cc), as evidenced by observation of the previously assigned bands ν_4 (1375 cm^{-1}), ν_3 (1505 cm^{-1}), ν_{10} (1640 cm^{-1}) and others (see Table 1).[11,31] In contrast, the spectrum for PEG-stabilized Cc:Au adsorbed to this substrate (Ag:Cc:Au) is dominated by nonheme bands (Supporting Information). Control experiments showed these bands to be related to the PEG stabilizer present in the Cc:Au solution.[54] After determining that stabilizers interfered with SERS acquisition, conjugates were prepared without them. For Cc:Au, stable conjugates could be prepared easily in the absence of such additives. For the remainder of this work, only stabilizer-free Cc:Au was used in SERS studies.

SERS spectra, at Ag aggregates, for Cc (**A**, Ag:Cc) and unstabilized Cc:Au conjugates (**B**, Ag:Cc:Au) are shown in Figures 3 (514.5-nm excitation) and 4 (568.2 nm excitation); see Chart 1 for the geometries of **A** and **B**. In these and subsequent figures, SERS spectra of Cc:Au conjugates are compared to those of the same concentration of Cc (as in the conjugate) adsorbed directly to aggregated Ag, under identical conditions. The Cc concentration in Ag:Cc and Ag:Cc:Au samples was equivalent.[55] Stated another way, the top and bottom parts of Figure 3 compare spectra for the same amounts of protein added to aliquots of the same aggregated Ag sol, excited at the same power (55 mW of 514.5 nm),[56] with an identical integration time. The only difference in the experiment is that for the spectrum labeled Ag:Cc:Au, the Cc was conjugated to colloidal Au, whereas the spectrum labeled Ag:Cc, the Cc was added directly. The top and bottom panels of Figure 4 are equally similar, except that the excitation wavelength is 568.2 nm.

The greater SERS signal for Ag:Cc (**A**) than for Ag:Cc:Au (**B**) in Figures 3 and 4 is due to the location of the Cc heme in the two geometries, and provides strong evidence that Cc does not desorb from Cc:Au. In **A**, the heme group is located very close to the Ag surface, while in **B**, the heme group is close to the *Au* surface and far from the Ag. Since the SERS effect drops off exponentially with distance from the Ag substrate,[2,29] much less signal is expected for the geometry shown in **B** than

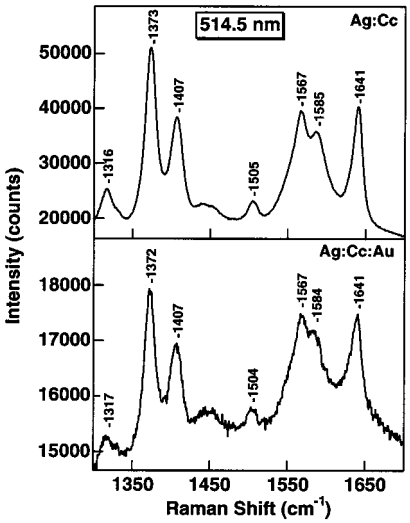

Figure 3. SERS for Ag:Cc (top) and Ag:Cc:Au (bottom) with 514.5-nm excitation. Conditions for both spectra: [Cc] = 7.5×10^{-8} M, 55 mW power at the sample, 30 s integration × 3 accumulations, 5 cm^{-1} band-pass.

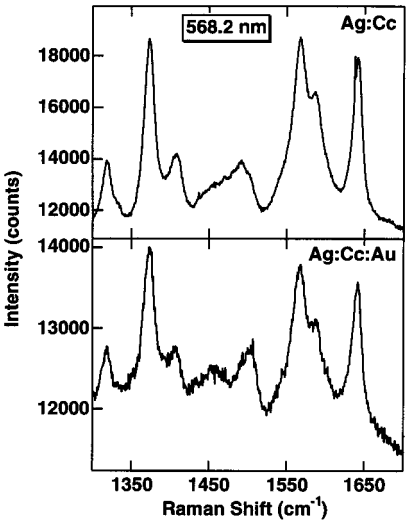

Figure 4. SERS for Ag:Cc (top) and Ag:Cc:Au (bottom) with 568.2 nm excitation. Conditions for both spectra: [Cc] = 5.8×10^{-8} M, 74 mW power at the sample, 30 s integration × 3 accumulations, 5 cm^{-1} band-pass.

A. Indeed, the *closest* heme−Ag distance in **B** is nearly the same as for the "buried" heme groups unobservable in SERS studies of the multiheme protein, cytochrome c_3.[28] Note that the SERS intensity differences observed at two different excitation wavelengths proves that Cc:Au remains intact upon adsorption. If Cc desorbed from the Au nanoparticles, it would be available for adsorption onto the aggregated Ag surface. Had all of the Cc desorbed and then bound to Ag, the two spectra in Figure 3 would be identical. If only a fraction of the Cc migrated to the Ag surface, the SERS intensity observed for Ag:Cc:Au samples would be lower than that for Ag:Cc, as is observed in Figure 3. However, with SERS enhancement coming only from the Ag surface, the relative intensities for the two samples would be independent of excitation wavelength. This is not observed: for $\lambda_{ex} = 568.2$ nm, the SERS intensity of signal for Ag:Cc:Au is closer to that for Ag:Cc (they differ by a factor of ~3), while at $\lambda_{ex} = 514.5$ nm, the SERS intensity for Ag:Cc greatly exceeds that for Ag:Cc:Au (they differ by a factor of ~10). (An explanation for this phenomenon is provided in the accompanying paper.[30]) The point is that

differences in relative intensities for Ag:Cc and Ag:Cc:Au at different excitation wavelengths argues strongly against dissociation of Cc in Cc:Au.

SERS spectra for Ag:Cc and Ag:Cc:Au are very similar in terms of band positions. Thus, conjugation to colloidal Au prior to adsorption at aggregated Ag does not perturb the conformation of Cc. Furthermore, the spectra for $\lambda_{ex} = 514.5$ nm (Figure 3) are essentially identical to those previously observed at citrate-reduced Ag sols,[18] and show no signs of Cc denaturation or conformational change at the surface. The location of the ν_4 vibration (oxidation state marker band) at 1375 cm^{-1} is consistent with ferriCc, while the location of the spin-state marker bands (e.g., ν_{10} at 1640 cm^{-1}) is consistent with a low-spin, 6-coordinate heme.[11,31] Cc SERS using 568.2 nm excitation has not appeared in the literature; however, most of the spectral differences between the Ag:Cc spectra excited at 568 nm and those with 514 nm excitation can be understood in terms of the wavelength dependence of Cc RR.[11,31,57] It should be noted that all of the spectra shown here report on the average heme environment and do not preclude the possibility that a small fraction of Cc at the surface has undergone conformational changes.[58]

Orientation of the Cc Heme in Metal−Cc−Metal Sandwiches. While it has been shown previously that the angle of Cc's heme with respect to the surface changes with Cc coverage,[18] Ag:Cc:Au retains its initial orientation at all Cc:Au coverages. Thus, a key advantage to the "conjugate approach" to protein SERS is that the conjugate can be made at one concentration relative to the carrier particle (i.e., colloidal Au) and the SERS measurement can be made at another. Moreover, the amount of protein required to make the conjugates is extremely low.

SERS selection rules[60] can be used in some cases to determine bond orientations with respect to the enhancing substrate.[61] For a heme chromophore having a symmetry of D_{4h} (typically taken as model for Cc heme, although in Cc the Fe axial ligands differ; the same arguments obtain for C_{4v}), both totally symmetric modes (e.g., the A_{1g} mode ν_4) and nontotally symmetric modes (e.g., the B_{1g} mode ν_{10}) involve motion along the *x*- and *y*- axes (in the plane of the porphyrin), while the totally symmetric (A_{1g}) modes involve displacement along the *x*, *y*, and *z* directions.[11a,31,62−64] The SERS effect preferentially enhances vibrations which involve a change in polarizability along an axis perpendicular to the surface.[60] Thus, B_{1g} modes would be expected to be large only when the heme in-plane vibrations have a large component perpendicular to the surface (that is, when the heme is "standing up"; in this orientation, A_{1g} modes are also expected to exhibit good enhancement. For a heme group laying flat on the surface, *only* A_{1g} modes are expected to scatter effectively. Thus, as the angle of the heme with respect to the surface normal increases, a relative increase in SERS intensity for totally symmetric modes over nontotally symmetric modes is predicted (i.e., the B_{1g}/A_{1g} SERS intensity ratio decreases).[65]

In practice, the relative intensity pattern observed in a SERS spectrum is due to a combination of several effects,[65] making quantitative predictions of bond orientations from a single spectrum nontrivial. For example, in the wavelength-dependent Cc SERS at aggregated Ag sols reported in the accompanying article,[30] the nontotally symmetric band ν_{10} increased relative to the totally symmetric ν_4 with increasing λ_{ex}; this result highlights the importance of the resonance contribution to Cc SERS. However, for spectra acquired at a *given* λ_{ex}, changes in the B_{1g}/A_{1g} (e.g., ν_{10}/ν_4) ratio are expected upon changes in the orientation of the heme moiety with respect to the surface.

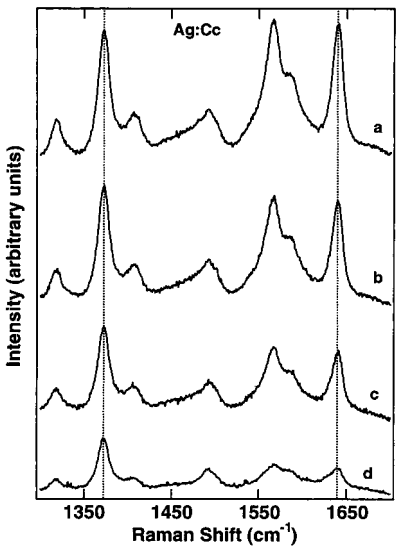

Figure 5. SERS spectra for Ag:Cc for several [Cc]: (curve a) 1.6×10^{-7} M, (curve b) 8.3×10^{-8} M, (curve c) 4.2×10^{-8} M, (curve d) 1.6×10^{-8} M. Conditions: 34 mW of 568.2-nm excitation; 90 s integration × 1 accumulation for a and b and × 3 accumulations for c and d; 5 cm^{-1} band-pass.

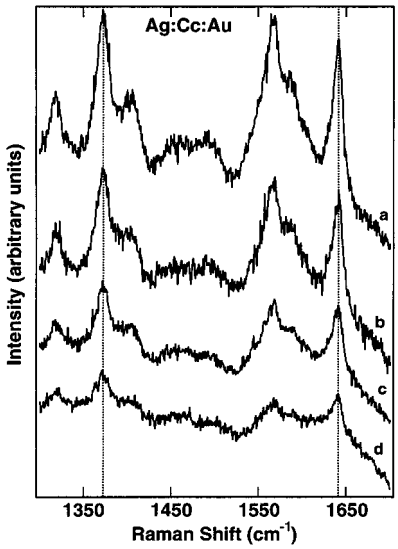

Figure 6. SERS spectra for Ag:Cc:Au for several [Cc]: (curve a) 8.3×10^{-8} M, (curve b) 4.2×10^{-8} M, (curve c) 2.1×10^{-8} M, (curve d) 8.3×10^{-9} M. Conditions: 34 mW of 568.2-nm excitation, 90 s integration × 1 accumulation for a and b and × 3 accumulations for c and d, 5 cm^{-1} band-pass.

SERS spectra with $\lambda_{ex} = 568$ nm for Cc adsorbed to aggregated colloidal Ag at various [Cc] are shown in Figure 5. The ν_4 (1375 cm^{-1}) and ν_{10} (1640 cm^{-1}) vibrations are indicated with dotted vertical lines. At the highest [Cc], 1.6×10^{-7} M, the ν_4 and ν_{10} vibrations are roughly equal in intensity. As the [Cc] decreases, the intensity of the ν_{10} band decreases relative to ν_4. In contrast, the relative intensities of ν_4 and ν_{10} in Ag:Cc:Au remain constant as [Cc:Au] is decreased over the same range of [Cc] (Figure 6). Figure 7 shows the ν_{10}/ν_4 intensity ratio for Ag:Cc and Ag:Cc:Au as a function of [Cc]. At high [Cc], there is sufficient Cc in the solution to completely coat the aggregated Ag surface, and this ratio is approximately equal for Ag:Cc and Ag:Cc:Au. As the [Cc] is decreased, however,

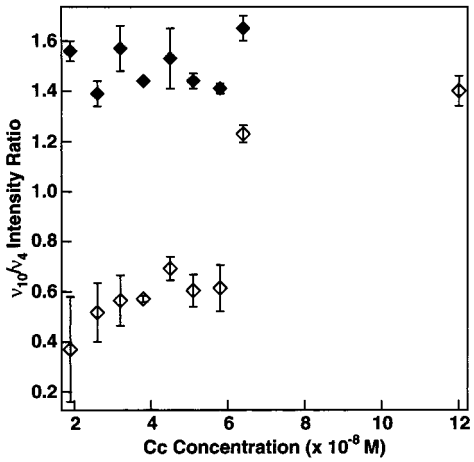

Figure 7. Average ν_{10}/ν_4 intensity ratio for Ag:Cc (open symbols) and Ag:Cc:Au (filled symbols), from several sets of data similar to that shown in Figures 5 and 6.

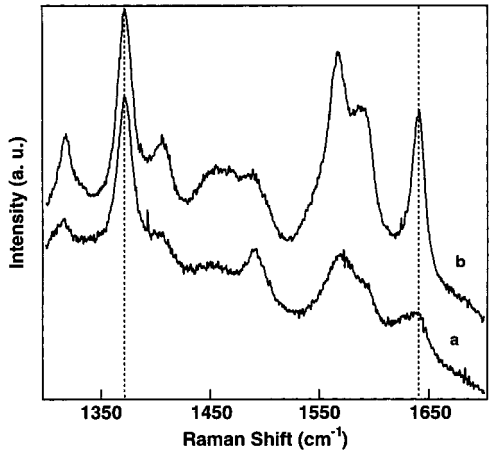

Figure 8. SERS spectra at 568.2 nm excitation, for Cc:Ag/Au conjugates prepared under (curve a) high [Cc], and (curve b) low [Cc] conditions (0.2 monolayer coverage). Conditions for both spectra: [Cc] $= 7.5 \times 10^{-8}$ M (the concentration of Cc:Ag/Au was altered to keep [Cc] constant), 54 mW power at the sample, 30 s integration $\times$ 3 accumulations, 5 cm^{-1} band-pass.

the ν_{10}/ν_4 ratio for Ag:Cc ratio drops sharply, while the ratio for Ag:Cc:Au remains unchanged.

MacDonald and Smith[18] have observed a change in the ν_{10}/ν_4 SERS intensity ratio in response to changes in [Cc] for Cc adsorbed to colloidal Ag aggregates. This result was interpreted in terms of changes in protein packing on the surface. At very low [Cc], the ν_{10}/ν_4 intensity ratio decreased, indicating that the angle between the heme plane and the surface normal had increased compared to its position at high packing densities, based on symmetry arguments as described above.[18] The reason for Cc's conformational change with surface coverage was proposed to be due to favorable protein−protein interactions at high Cc densities.[18] Illustrations **A** and **C** in Chart 1 highlight the difference in Cc orientation on Ag at high and low coverage, respectively. In contrast, the Cc:Au conjugates used in Ag:Cc:Au samples are prepared under high Cc packing conditions, and the number of Cc per Au particle does not change upon dilution of the Cc:Au added to aggregated Ag sol. Thus, the Cc concentration on the colloidal Au is fixed, irrespective of the amount of Cc:Au added to aggregated Ag.

Figure 8 compares SERS spectra at aggregated Ag for Cc:nanoparticle conjugates which were prepared at high and low [Cc]. Spectrum a represents conjugate with a monolayer of Cc adsorbed to the surface, while spectrum b is for a conjugate prepared with only enough Cc for 0.2 monolayer coverage. As expected, there is a dramatic difference in ν_{10}/ν_4 ratio. Beyond this, the data are revealing in two respects. (i) When the low-coverage conjugates were prepared, the Cc partially coated all of the Au particles, rather than fully coating only some; had full coating occurred, the ν_{10}/ν_4 ratio for a and b would be the same. (ii) The Cc conformation determined by the initial [Cc] present during conjugate formation was retained for low Cc coverages as well as high coverages. This is further evidence that Cc cannot desorb from metal nanoparticles after preparation of conjugates. The results of this experiment suggest that it should be possible to use conjugates to control protein orientation, by dictating their concentration during conjugate formation. Importantly, this technique can also be coupled with manipulation of the protein:Au binding chemistry through, for example, covalent modification of protein residues.[67]

Protein Stability in Metal−Cc−Metal Sandwiches. Prior conjugation to colloidal Au prevents the evolution of non-native spin states in Cc under conditions sufficient to cause them in free Cc of the same concentration. Hildebrandt and Stockburger have observed that Cc adsorbed at SERS-active Ag electrodes existed in a mixed spin-state at room temperature, but could be reversibly converted to the native low-spin state by lowering the temperature to 196 K.[32] Based on the reversibility of this conversion, they concluded that the protein had not denatured but had instead undergone a surface-induced, reversible conformational change at higher temperatures. Further experiments on Cc adsorbed at negatively charged surfaces of Ag sols, Ag electrodes, tungstate salts, and phospholipid bilayers have indicated the presence of two populations of Cc at the interface.[33] Although Cc itself is found in solution, its physiological role is to shuttle electrons between two membrane-bound proteins. Thus, Cc-surface interactions may be functionally significant. Hildebrandt and co-workers found evidence for the presence of two distinct conformations of Cc bound to surfaces and refer to these as states I and II. In state I, the protein has not undergone significant structural changes at the surface, while in state II, SERS data show the onset of a mixed-spin state population and an "opening" of the heme pocket.[68]

Conversions from Cc's native low spin (LS) to high spin (HS) have been observed previously at citrate-reduced Ag sols for low [Cc].[18] To assess the extent of conversion from low spin to high spin in conjugates, SERS spectra at 568.2 nm excitation for free Cc and Cc:Au adsorbed to aggregated Ag sols were acquired at various times after sample preparation. The samples were exposed to the laser beam only during spectral acquisition. The [Cc] in the first set of samples was 1.7×10^{-8} M, which is less-than-monolayer coverage on the aggregated Ag substrate. The free Cc sample begins to show some spectral changes (i.e., changes in the ratios of bands) after only 15 min, while the Cc:Au spectrum remains essentially unchanged, other than an overall increase in intensity, for more than 45 min (Supporting Information). The increase in intensity over time is not related to errors in sample positioning, which is very reproducible. Rather, it results from slow, time-dependent changes in aggregation of colloidal Ag. This phenomenon, which occurs over ~0.5 hour, occurred for all compounds, irrespective of the presence or absence of colloidal Au. Accordingly, care was taken to run samples at identical times after aggregation in this experiment, and more generally, immediately after sample preparation. The spectral changes observed for Ag:Cc are due to a partial LS to HS conversion, as evidenced by the loss of intensity for the spin state marker band, ν_{10}, at 1640 cm^{-1}, and

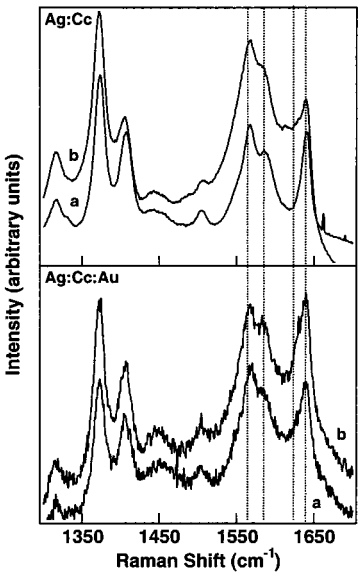

Figure 9. Stability of free Cc (top) vs Cc:Au (bottom) on aggregated Ag sols toward spin state conversions. Spectra were taken at 0 min (curve a), and 120 min (curve b), after preparation of SERS sample. Samples were illuminated with laser light only during spectral acquisition. Conditions: 55 mW of 514.5 nm excitation, [Cc] = 7.5×10^{-8} M, 30 s integration × 3 accumulations, 5 cm^{-1} band-pass.

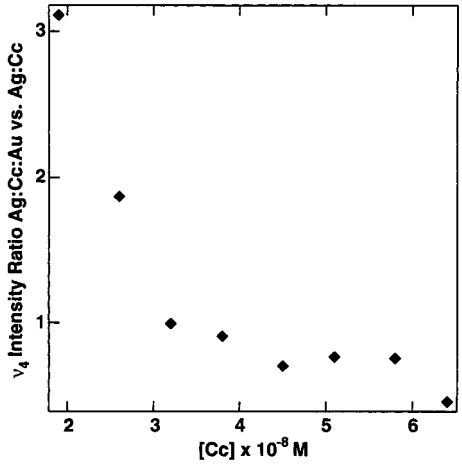

Figure 10. ν_4 SERS intensity ratio at 568.2 nm excitation for Ag:Cc:Au versus Ag:Cc as a function of [Cc].

the gain of intensity for this mode at ~1630 cm^{-1}. The enhanced stability of Cc conjugated to colloidal Au can be attributed to the restricted conformational flexibility of the close-packed Cc molecules of the Cc:Au as compared to the low coverage Cc adsorbed directly to colloidal Ag aggregates.

Ag:Cc:Au also exhibits increased stability relative to Ag:Cc at higher concentrations. SERS spectra for Cc and Cc:Au at [Cc] = 7.5×10^{-8} M, acquired 120 min after sample preparation, are shown in Figure 9. The Cc:Au sample is essentially unchanged, while the Cc shows clear signs of conformational changes indicative of some high-spin Fe in the sample (see above). Thus, even at higher Cc coverages, prior conjugation to colloidal Au has increased the resistance of adsorbed Cc to conformational changes that can lead to denaturation. This could be due to the still somewhat denser packing of Cc in Ag:Cc:Au as compared to Ag:Cc, to the smaller radius of curvature of the 12-nm Au spheres as compared to the Ag aggregates, or to a combination of these effects. Whatever the cause of this added stability, it illustrates a clear advantage to the use of Au conjugates for protein SERS.

Another advantage to conjugate SERS was the reduced rate of protein loss due to adsorption to container walls. Figure 10 is a plot of the ν_4 SERS intensity ratio for Ag:Cc:Au vs Ag:Cc as a function of [Cc]. It was observed during these studies that dilute Cc solutions stored for several hours in either glass vials or plastic microcentrifuge tubes lost a substantial amount of Cc from solution over time. Presumably the missing Cc had bound to the vessel walls. For Cc:Au at similar concentrations, no change in concentration was observed over the same time periods. Accordingly, the ratio increased at low concentrations, with Ag:Cc:Au yielding more intense spectra than Ag:Cc as the overall [Cc] fell below 30 nM. This phenomenon could be due to the much slower diffusion for Cc-clad Au nanoparticles or to blocking of adsorption sites on the Cc by the Au (e.g., if the free Cc bound to the vessel walls through the lysine patch, which was already bound to Au in the conjugates).

Conclusions

Stable conjugates of Cc to 12-nm Au have been prepared. Adsorption of Cc:Au to aggregated Ag does not lead to desorption of Cc. The normal dependence of SERS intensity with increasing distance from the (aggregated Ag) substrate is overcome by positioning the analyte between two metal structures. This should allow investigation of biomolecules having "buried" chromophores. Cc orientation can be altered by changing the concentration at which conjugates are prepared; this orientation is retained upon exposure of conjugates to high salt solutions and colloidal Ag aggregates, and is independent of conjugate concentration. Cc:Au conjugates adsorbed to aggregates of colloidal Ag have been shown to exhibit greater stability to conformational and spin-state changes than Cc directly adsorbed to Ag aggregates. Additionally, increased enhancement factors are possible for protein molecules sandwiched between carrier metal nanoparticles and the Ag surface.[30]

Acknowledgment. We are indebted to Ken Brown for chromatographic purification of horse heart cytochrome *c*, and to Prof. W. DeW. Horrocks and his research group for the use of the micro centrifuge. Support from NSF (Grant CHE-9627338), NIH (Grants GM55312-01 and DK48784-01A2), the Henkel Corporation/ACS Division of Colloid and Surface Chemistry (through a graduate fellowship to C.D.K.), and the Penn State Department of Chemistry (through a Teas Scholarship to K.M.K.) is gratefully acknowledged. Acknowledgment is also made to the Electron Microscopy Facility for the Life Sciences in the Biotechnology Institute at The Pennsylvania State University.

Supporting Information Available: Flocculation data for Cc binding to 40-nm and 60-nm diameter colloidal Au, SERS spectra for PEG-stabilized Cc:Au, SERS spectra of Ag:Cc and Ag:Cc:Au (568.2 nm excitation) at $t = 0$ and 45 min (4 pages total). Ordering information is given on any current masthead page.

References and Notes

(1) (a) Scott, R. A., Mauk, A. G., Eds. *Cytochrome c*: *A Multidisciplinary Approach*; University Science Books: Sausalito, CA, 1996. (b) Lever, A. B. P., Gray, H. B., Eds. *Iron Porphyrins*; Addison-Wesley: Reading, MA, 1983 (in two volumes). (c) Moore, G. R., Pettigrew, G. W., Eds. *Cytochromes c: Evolutionary, Structural and Physicochemical Aspects*; Springer-Verlag: Berlin, 1990.

(2) (a) Brandt, E. S.; Cotton, T. M. In *Investigations of Surfaces and Interfaces-Part B*, 2nd ed.; Rossiter, B. W., Baetzold R. C., Eds.; John Wiley & Sons: New York, 1993; Chapter 8. (b) Garrell, R. L. *Anal. Chem.* **1989**, *61*, 410A-411A. (c) Campion, A. in *Vibrational Spectroscopy of Molecules*

on Surfaces; Yates, J. T., Jr., Madley, T. E. M., Eds., Plenum: New York, 1987; pp 345−415.

(3) Crumbliss, A. L.; Stonehuerner, J. G.; Henkens, R. W. *Biosens. Bioelectron.* **1993**, *8*, 331−337.

(4) Yeong, D.; Gill, A.; Maule, C. H.; Davies, R. J. *Trends Anal. Chem*. **1995**, *14*, 49−56.

(5) Buttry, D. A.; Ward, M. D. *Chem. Rev*. **1992**, *92*, 1355−1379.

(6) (a) Sadana, A. *Chem. Rev*. **1992**, *92*, 1799−1818. (b) Yang, M.; Chung, F. L.; Thompson, M. *Anal. Chem*. **1993**, *65*, 3713−3716. (c) Williams, D. F., Ed. *Fundamental Aspects of Biocompatibility*; CRC Press: Boca Raton, FL, 1981.

(7) (a) Hobara, D.; Niki, K.; Zhou, C.; Chumanov, G.; Cotton, T. M. *Colloids Surf. A: Physicochem. Eng. Aspects* **1994**, *93*, 241−250. (b) Song, S.; Clark, R. A.; Bowden, E. F.; Tarlov, M. J. *J. Phys. Chem*. **1993**, *97*, 6564−6572. (c) Armstrong, F. A.; Cox, P. A.; Hill, H. A. O.; Oliver, B. N.; Williams, A.; A. *J. Chem. Soc., Chem. Commun*. **1985**, 1236−1237. (d) Eddowes, M. J.; Hill, H. A. O. *J. Am. Chem. Soc*. **1979**, *101*, 4461−4464.

(8) Löfas, S. *Pure Appl. Chem.* **1995**, *67*, 829−834.

(9) Brown, K. R.; Fox, A. P.; Natan, M. J. *J. Am. Chem. Soc*. **1996**, *118*, 1154−1157.

(10) Hayat, M. A., Ed., *Colloidal Gold: Principles, Methods, and Applications*; Academic Press: New York, 1989 (in three volumes).

(11) (a) Spiro, T. G., Ed. *Biological Applications of Raman Spectroscopy*; John Wiley & Sons: New York, 1988; Vol. 3. (b) Wang, Y.; Van Wart, H. E. In *Methods in Enzymology*; Riordan, J. F., Vallee, B. L., Eds.; Academic Press: San Diego, 1993; Vol. 226, pp 319−373. (c) Spiro, T. G.; Czernuszewicz, R. S. In *Methods in Enzymology*; Sauer, K., Ed.; Academic Press: San Diego, 1995; Vol. 246, pp 416−460.

(12) (a) Hildebrandt, P.; Stockburger, M. *J. Phys. Chem*. **1984**, *88*, 5935−5944. (b) Weitz, D. A.; Garoff, S.; Gersten, J. I.; Nitzan, A. *J. Chem. Phys*. **1983**, *78*, 5324−5338.

(13) (a) Smith, W. E. In *Methods in Enzymology*; Riordan, J. F., Vallee, B. L., Eds.; Academic Press: San Diego, 1993; Vol. 226, pp 319−373. (b) Cotton, T. M.; Kim, J.-H.; Chumanov, G. D. *J. Raman Spectrosc*. **1991**, *22*, 729−742.

(14) (a) Beer, K. D.; Tanner, W.; Garrell, R. L. *J. Electroanal. Chem*. **1989**, *258*, 313−325. (b) Barz, F.; Gordon, J. G., II; Philpott, M. R.; Weaver, M. J. *Chem. Phys. Lett*. **1983**, *94*, 168−171. (c) Jeanmarie, D. L.; Van Duyne, R. P. *J. Electroanal. Chem*. **1977**, *84*, 1−20.

(15) (a) Sanchez-Cortez, S.; Garcia-Ramos, J. V.; Morcillo, *J. Colloid Interface Sci*. **1994**, *167*, 428−436. (b) Heard, S. M.; Greieser, F. J.; Barraclough, C. G. *J. Colloid Interface Sci*. **1983**, *93*, 545−555. (c) Blatchford, C. G.; Campbell, J. R.; Creighton, J. A. *Surf. Sci*. **1982**, *120*, 435−455. (d) Creighton, J. A.; Blatchford, C. G.; Albrecht, M. G. *J. Chem. Soc., Faraday Trans*. **1979**, *75*, 790−798.

(16) (a) Smulevich, G.; Spiro, T. G. *J. Phys. Chem*. **1985**, *89*, 5168−5173. (b) Holt, R. E.; Cotton, T. M. *J. Am. Chem. Soc*., **1987**, *109*, 1841−1845.

(17) Broderick, J. B.; Natan, M. J.; O'Halloran, T. V.; Van Duyne, R. P. *Biochemistry* **1993**, *32*, 13771−13776.

(18) MacDonald, I. D. G.; Smith, W. E. *Langmuir* **1996**, *12*, 706−713.

(19) Rospendowski, B. N.; Kelly, K.; Wolf, C. R.; Smith, W. E. *J. Am. Chem. Soc*. **1991**, *113*, 1217−1225.

(20) Bright, R. B.; Musick, M. D.; Natan, M. J. *Langmuir* **1998**, *14*, 5695−5701.

(21) (a) Turkevich, J.; Stevenson, P. C.; Hillier, J. *Discuss. Faraday Soc*. **1951**, *11*, 55−75. (b) Frens, G. *Nature Phys. Sci*. **1973**, *241*, 20−22.

(22) (a) De Roe, C.; Courtoy, P. J.; Baudhuin, P. *J. Histochem. Cytochem*. **1987**, *35*, 1191−1198. (b) Polak, J. M., Van Noorden, S., Eds.; *Immunocytochemistry*; Wright: London, 1983.

(23) Geoghegan, W. D.; Ackerman, G. A. *J. Histochem. Cytochem*. **1977**, *25*, 1187−1200.

(24) Zeman, E. J.; Schatz, G. C. *J. Phys. Chem*. **1987**, *91*, 634−643.

(25) Ahern, A. M.; Garrell, R. L. *Langmuir* **1991**, *7*, 254−261.

(26) (a) Xu, J.; Birke, R. L.; Lombardi, J. R. *J. Am. Chem. Soc*. **1987**, *109*, 5645−5649. (b) Lee, N.-S.; Sheng, R.-s.; Morris, M. D.; Schopfer, L. M. *J. Am. Chem. Soc*. **1986**, *108*, 6179−6183.

(27) (a) Lee, N.-S.; Hsieh, Y.-Z.; Morris, M. D.; Schopfer, L. M. *J. Am. Chem. Soc*. **1987**, *109*, 1358−1363. (b) Holt, R. E.; Cotton, T. E. *J. Am. Chem. Soc*. **1987**, *109*, 1841−1845.

(28) (a) Eng, L. H.; Schlegel, V.; Wang, D.; Neujahr, H. Y.; Stankovich, M. T.; Cotton, T. *Langmuir* **1996**, *12*, 3055−3059. (b) Niki, K.; Kawasaki, Y.; Kimura, Y.; Higuchi, Y.; Yasuoka, N. *Langmuir* **1987**, *3*, 982−986.

(29) (a) Ye, Q.; Fang, J.; Sun, L. *J. Phys. Chem. B* **1997**, *101*, 8221−8224. (b) Tsen, M.; Sun, L. *Anal. Chim. Acta* **1995**, *307*, 333−340. (c) Cotton, T. M.; Uphaus, R. A.; Mobius, D. *J. Phys. Chem*. **1986**, *90*, 6071−6073. (d) Kovacs, G. J.; Luotfy, R. O.; Vincett, P. S.; Jennings, C.; Aroca, R. *Langmuir* **1986**, *2*, 689−694.

(30) Keating, C. D.; Kovaleski, K. M.; Natan, M. J. *J. Phys. Chem. B* **1998**, *102*, 9414.

(31) (a) Hildebrandt, P. In *Cytochrome c*: *a Multidisciplinary Approach*; Scott, R. A., Mauk, A. G., Eds.; University Science Books: Sausalito, CA, 1996; Chapter 6. (b) Cartling, B. *Biophys. J*. **1983**, *43*, 191−205.

(32) Hildebrandt, P.; Stockburger, M. *J. Phys. Chem*. **1986**, *90*, 6017−6024.

(33) (a) Hildebrandt, P.; Stockburger, M. *Biochemistry* **1989**, *28*, 6710−6721. (b) Hildebrandt, P.; Stockburger, M. *Biochemistry* **1989**, *28*, 6722−6728. (c) Hildebrandt, P.; Stockburger, M. *J. Phys. Chem*. **1986**, *90*, 6017−6024.

(34) (a) Niaura, G.; Gaigalas, A. K.; Vilker, V. L. *J. Electroanal. Chem*. **1996**, *416*, 167−178. (b) Sibbald, M. S.; Chumanov, G.; Cotton, T. M. *J. Phys. Chem*. **1996**, *100*, 4672−4678. (c) Maeda, Y.; Yamamoto, H.; Kitano, H. *J. Phys. Chem*. **1995**, *99*, 4837−4841.

(35) Hu, S.; Morris, I. K.; Singh, J. P.; Smith, K. M.; Spiro, T. G. *J. Am. Chem. Soc*. **1993**, *115*, 12446−12458.

(36) Bushnell, G. W.; Louie, G. V.; Breyer, G. D. *J. Mol. Biol.* **1990**, *214*, 585−595.

(37) (a) Edmiston, P. L.; Lee, J. E.; Cheng, S.-S., Saavedra, S. S. *J. Am. Chem. Soc*. **1997**, *119*, 560−570. (b) Lee, J. E.; Saavedra, S. S. *Langmuir* **1996**, *12*, 4025−4032. (c) Heimburg, T.; Hildebrandt, P.; Marsh, D. *Biochemistry* **1991**, *30*, 9084−9089. (d) Hildebrandt, P. *J. Mol. Struct.* **1991**, *242*, 379−395.

(38) Brautigan, D. L.; Ferguson-Miller, S.; Margoliash, E. In *Methods in Enzymology*; Fleischer, S., Packer, L., Eds.; Academic Press: San Diego, 1978; Vol. 53, pp 128−164.

(39) Lee, P. V.; Meisel, D. *J. Phys. Chem*. **1982**, *86*, 3391−3395.

(40) Grabar, K. C.; Freeman, R. G.; Hommer, M. B.; Natan, M. J. *Anal. Chem.* **1995**, *267*, 1629−1632.

(41) Available on the Internet at zippy.nimh.nig.gov by anonymous FTP.

(42) Schutt, E. G. Eur. Pat. Appl. 90317671.4, Sept. 25, 1990.

(43) Brown, K. R.; Natan, M. J. *Langmuir* **1998**, *14*, 726−728.

(44) Freeman, R. G.; Hommer, M. B.; Grabar, K. C.; Jackson, M. A.; Natan, M. J. *J. Phys. Chem*. **1996**, *100*, 718−724.

(45) Throughout the manuscript, the following notation will be used: M_1:Cc: M_2, where M_1 refers to the aggregated colloidal metal substrate and M_2 refers to the metal nanoparticle to which Cc has been previously conjugated. For example, Ag:Cc:Au refers to Cc:Au conjugates adsorbed at the surface of aggregated Ag nanoparticles. Ag: Cc refers to Cc added directly to aggregated colloidal Ag, without first adsorbing it to Au particles.

(46) (a) Quinten, M.; Kreibig, U. *Surf. Sci*. **1986**, *172*, 557−577. (b) Kreibig, U.; Vollmer, M. *Optical Properties of Metal Clusters*; Springer-Verlag: Berlin, 1995.

(47) (a) Hunter, R. J. *Introduction to Modern Colloid Science*; Oxford University Press: New York, 1993. (b) Schmid, G., Ed. *Colloids and Clusters*; VCH: New York, 1994.

(48) This absorbance is expected to decrease with particle aggregation, but not to disappear completely, since the transverse mode of the collective particle oscillations is also located in this region.[46]

(49) Heard, S. M.; Greieser, F. J.; Barraclough, C, G. *J. Colloid Interface Sci*. **1983**, *93*, 545−555.

(50) A slight shift in the position of the absorbance maximum is expected upon protein binding, due to the change in the dielectric at the surface of the particle (For example, see: Underwood, S.; Mulvaney, P. *Langmuir* **1994**, *10*, 3427−3430.).

(51) Stabilizers were observed in TEM images of the particles (data not shown).

(52) Frens, G. *Kolloid−Z. Z. Polym.* **1972**, *250*, 736−741.

(53) Kerker, M.; Siiman, O.; Bumm, L. A.; Wang, D.-S. *Appl. Opt*. **1980**, *19*, 3253−3255.

(54) No vibrations attributable to heme are observed for PEG-stabilized Cc:Au at 647.1- or 488.0-nm excitation (data not shown). For 568.2 nm excitation, however, weak heme vibrations are observable in the PEG-stabilized Cc: Au SERS at aggregated Ag (Supporting Information).

(55) Actually, type **A** samples are expected to contain ∼10% more Cc than type **B**, since the excess Cc in Cc:Au conjugates is expected to have been removed in the centrifugation/resuspension step.

(56) Ag:Cc and Ag:Cc:Au samples were freshly prepared and run one immediately after the other, with no change in beam steering or collection optics, so that they could be directly compared.

(57) The principle differences between the SERS spectra acquired with $\lambda_{ex} = 514.5$ nm (Figure 3) and those acquired with $\lambda_{ex} = 568.2$ nm (Figure 4) are in the 1400−1550 cm^{-1} region. At $\lambda_{ex} = 568.2$ nm, the band at ∼1450 cm^{-1} exhibits increased intensity, and the ∼1505-cm^{-1} band (assigned as the ν_3 vibrational mode) has given way to one at ∼1490 cm^{-1} in both Ag:Cc and Ag:Cc:Au spectra. A shift in ν_3 from 1505- to 1490 cm^{-1} has been correlated with conversion to high-spin heme, which, for Cc, often involves the loss of an axial ligand.[11a,31] Thus, one interpretation of the spectra shown in Figure 4 is that the Cc has denatured at the Ag surface. However, shifts in the other spin state marker band (ν_{10}) are not observed, suggesting the need for an alternate explanation. All Ag:Cc or Ag:Cc:Au samples prepared have shown a band at 1505 cm^{-1} when excited at 514.5 nm, and all have shown some intensity ∼1490 cm^{-1} (and no band

at ~1505 cm^{-1}) when excited at 568.2 nm. In addition, the shape of the 1450−1500-cm^{-1} region for $\lambda_{ex} = 568.2$ nm is somewhat variable between samples; this might indicate slight differences in protein conformation for which the 568.2-nm excitation spectrum is more sensitive than for 514.5-nm excitation. Because these spectral features (loss of ν_3 band at 1505-cm^{-1}, gain in intensity ~1490 cm^{-1}) are unobservable at any other λ_{ex} tested, it is unlikely that ν_3 is the correct assignment for the 1490-cm^{-1} band seen in Cc SERS spectra excited at 568.2 nm. Changes in band relative intensities with different λ_{ex} are expected for Cc RR.[11a,31] The disappearance of the 1505-cm^{-1} vibration at $\lambda_{ex} = 568.2$ nm is unsurprising because the ν_3 band has A_{1g} symmetry; thus, like ν_4, it is preferentially enhanced by excitation resonant or preresonant with the Soret absorbance (A term scattering). Excitation into the Q-bands of Cc leads to more effective scattering by nontotally symmetric modes, which can gain intensity by vibronic mixing (B term scattering). Thus, the new band at ~1490 cm^{-1} in $\lambda_{ex} = 568.2$ nm spectra may arise from vibrations not observable with standard excitations, either because of its symmetry (e.g., nontotally symmetric), or its origin (e.g., perhaps it is a protein-based rather than a heme-based mode).

(58) All bulk SERS measurements, because they interrogate many molecules, report only on the average orientation of molecules. A notable exception in the SERS literature is recent work by Nie and Emory showing single molecule SERS for rhodamine 6G adsorbed to isolated Ag particles.[59]

(59) Nie, S.; Emory, S. R. *Science* **1997**, *275*, 1102−1106.

(60) (a) Creighton, J. A. In *Spectroscopy of Surfaces;* Clark, R. J., Hester, R. P., Eds.; Wiley: New York, 1988; pp 37−89. (b) Moskovits, M. *J. Chem. Phys*. **1982**, *77*, 4408−4416.

(61) (a) Pemberton, J. E.; Bryant, M. A.; Sobocinski, R. L.; Joa, S. L. *J. Phys. Chem.* **1992**, *96*, 3776−3782. (b) Gao, X.; Davies, J. P.; Weaver, M. J. *J. Phys. Chem*. **1990**, *94*, 6858−6864. (c) Moskovits, M.; Suh, J. S. *J. Phys. Chem.* **1984**, *88*, 5526−5530. (d) Creighton, J. A. *Surf. Sci*. **1983**, *124*, 209−219.

(62) Due to the rhombic distortion of the heme in Cc, the actual symmetry is lower even than C_{4v}, making C_s a better model.[63] However, the normal-mode analysis for Ni octaethylporphyrin (NiOEP, see ref 64), which has been the basis for all heme chromophore band assignments, initially treated the ethyl substituents as point masses, such that NiOEP had D_{4h} symmetry; the labels have been carried over to molecules of lower symmetry. Nonetheless, the same arguments apply for Cc's heme, since the ν_{10} mode involves in-plane displacement while the ν_4 mode has both in-plane and out-of-plane components.

(63) Cotton, F. A. *Chemical Applications of Group Theory*, 3rd ed.; Wiley: New York, 1990.

(64) (a) Kitagawa, T.; Abe, M.; Ogoshi, H. *J. Chem. Phys.* **1978**, *69*, 4516−4525. (b) Abe, M.; Kitagawa, T.; Kyogoku, Y. *J. Chem. Phys*. **1978**, *69*, 4526−4534.

(65) The surface selection rules are most valid at long wavelengths (i.e., infrared) for several reasons. First, since metals have higher electrical conductivities at IR frequencies, the parallel (but not the perpendicular) electric field component of radiation goes to zero at the surface.[60] However, since SERS experiments typically employ visible excitation (where substrates are poorer conductors), the nontotally symmetric modes are not expected to disappear completely even if they involve no change in polarizability perpendicular to the surface. Second, for Cc SERS, use of excitation wavelengths near the intense Soret absorption band (404 nm) favors contribution from resonance enhancement over surface enhancement. Excitation into the Soret band (404 nm) leads to A-term scattering, which favors totally symmetric modes, while excitation into the weaker Q-bands (530−550 nm) leads to B-term scattering, whereby the nontotally symmetric bands (which gain intensity through vibronic coupling) are favored.[31,66] Thus, changing from 400- to 550-nm excitation, for example, should lead to a relative increase in B_{1g} modes over A_{1g} modes.

(66) (a) Shelnutt, J. A.; Cheung, L. D.; Chang, R. C. C.; Yu, N.-T.; Felton, R. H. *J. Chem. Phys*. **1977**, *66*, 3387−3398. (b) Shelnutt, J. A.; O'Shea, D. C.; Yu, N.-T.; Cheung, L. D.; Felton, R. H. *J. Chem. Phys*. **1976**, *64*, 1156−1165.

(67) (a) Wood, L. L.; Cheng, S.-S.; Edminston, P. L.; Saavedra, S. S. *J. Am. Chem. Soc*. **1997**, *119*, 571−576. (b) Firestone, M. A.; Shank. M. L.; Sligar, S. G.; Bohn, P. W. *J. Am. Chem. Soc*. **1996**, *118*, 9033−9041. (c) Jiang, M.; Nolting, B.; Stayton, P. S.; Sligar, S. G. *Langmuir* **1996**, *12*, 1278−1283.

(68) Such gross surface-induced conformational changes were not observed in the present study, nor in the work of MacDonald and Smith.[18] A principle difference between these studies and those of Hildebrandt appears to be not only the choice of substrate (the latter two studies have used citrate-reduced Ag sols), but also the surface concentration of adsorbed Cc. Although the Cc coverage is difficult to know precisely at the ill-defined roughened Ag surfaces used for SERS experiments, Hildebrandt and Stockburger estimated by Frumkin isotherm a coverage of only ~0.2 monolayer at a roughened Ag electrode.[32] Higher coverages of Cc were used in both the present work and in ref 18 (as evidenced by the greater ν_{10}/ν_4 ratio in the Cc SERS spectra at $\lambda_{ex} = 514.5$ nm).